ANALYSIS OF QUENCHANT UNIFORMITY USING COMPUTATIONAL FLUID DYNAMICS (CFD)

Geraldo Severi Junior, gjr.severi@gmail.com
Lauralice de Campos Franceschini Canale, lfcanale@sc.usp.br
Engineering School of São Carlos, University of São Paulo (EESC-USP)
Av. Trabalhador São-carlense, 400 – 13566-590 – São Carlos, SP – Brazil

Paulo Celso Greco Junior, pgreco@sc.usp.br
Engineering School of São Carlos, University of São Paulo (EESC-USP)
Av. Trabalhador São-carlense, 400 – 13566-590 – São Carlos, SP – Brazil

Abstract. *Quenching is performed to enhance mechanical properties such as hardness and strength. These characteristics are important to assure material workability resulting in improved reliability and durability of the final product. Various quench process parameters affect final as-quenched material properties including: the specific quenching medium used (oil, water and polymer and salt solutions), quenchant temperature and others. However, one of the most critical parameters is agitation which affects the uniformity of the flow field around the material during the quenching process which then affects the uniformity of heat transfer and ultimately material distortion control and potential for quench crack formation. Until recently, however, analysis of quench uniformity has not been routinely performed either in quench system design or in process troubleshooting due to the relative unavailability of software and adequate and cost-effective computation speeds required. However, with recently available improved computational codes and relatively low-cost desktop computers on which Computational Fluid Dynamics (CFD) analysis may be routinely performed, this important methodology is being used increasingly in the heat treating industry. This paper describes the use of CFD analysis to aid in the design of a laboratory agitation system for quenching studies.*

Keywords*: quench, uniformity, fluid flow, CFD.*

1. INTRODUCTION

1.1. Quench process

Properties such as hardness, strength, ductility, and toughness are dependent on the microstructural products that are present in steel (Narazaki et al., 2002). The first step in the transformation process is to heat the steel to its austenitizing temperature. The steel is then cooled sufficiently fast to avoid the formation of pearlite, which is a relatively soft transformation product, and to maximize formation of martensite, a relatively hard transformation product to achieve the desired as-quenched hardness. A Time-Temperature-Transformation (TTT) diagram illustrates these phase changes during the cooling process. An example of a TTT diagram is shown on the left-hand side. of Fig. 1.

During the quench process, and relative to the high temperature difference between quenchant and material, there are three distinct phases which are shown on right side of Fig. 1.

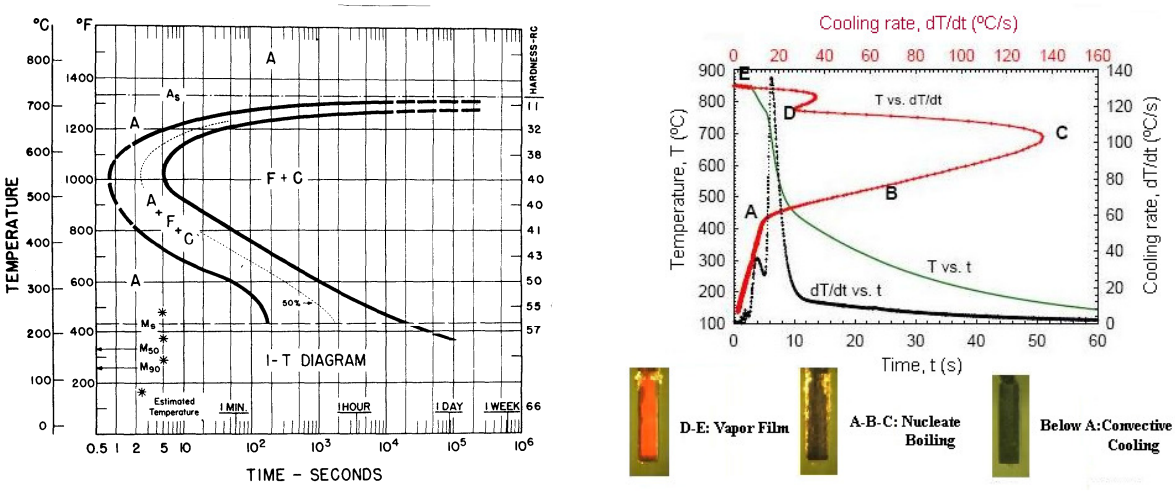

Figure 1. Example of a TTT diagram (ASM, 1977), on left-hand side, and a Cooling mechanism of a Quench process (Rondeau, 2006), on right side

Upon initial immersion, the metal undergoes a slow cooling process which is attributable to the vapor film surrounding the hot metal surface and the vaporizable liquid quenchant. The vapor phase may be suppressed by

agitation and/or changing the quenchant to an aqueous salt solutions. After further cooling, vapor film ruptures (at the Leidenfrost temperature) resulting in a nucleate boiling process which is the fastest cooling phase. After the metal surface reaches the boiling point of the quenchant, nucleate boiling stops and convective cooling begins.

Quenchants and quenching conditions must be selected to provide cooling rates capable of producing an acceptable microstructure in the section thickness of interest. There are many quench-related factors that affect distortion including the quenchant, flow rate, temperature of the quenchant, quench tank geometry, flow direction and turbulence. All of these parameters impact the quality of flow around a part during the quench (Funatani, 2003a, 2003b).

The objective of the quenching process is generally to maximize martensitic microstructure in steel by providing high cooling rates. This is accomplished varying parameters such as agitation, quenchant and quench bath temperature. In this paper, the use of computational fluid dynamics (CFD) will used to gain an insight into the impact of these parameters on the quality of flow in a model laboratory quench tank.

1.2. Computational Fluid Dynamics (CFD)

CFD codes are structured around the numerical algorithms that are used to address fluid flow problems and which include analysis of heat transfer and associated phenomena, such as chemical reactions and multiphase flow. The technique is very powerful and spans a wide range of industrial and non-industrial applications areas (Versteeg and Malalasekera, 1995).

Basically, CFD uses numerical methods to solve three fundamental physical equations: mass conservation, momentum conservation (Newton's second law), and energy conservation. These equations are manipulated by partial differential form, presented below (Anderson, 1995).

$$\frac{\partial \rho}{\partial t} + \nabla.(\rho V) = 0 \tag{1}$$

$$\frac{\partial(\rho u)}{\partial t} + \nabla.(\rho u V) = -\frac{\partial p}{\partial x} + \frac{\partial \tau_{xx}}{\partial x} + \frac{\partial \tau_{yx}}{\partial y} + \frac{\partial \tau_{zx}}{\partial z} + \rho f_x \tag{2}$$

$$\frac{\partial(\rho v)}{\partial t} + \nabla.(\rho v V) = -\frac{\partial p}{\partial y} + \frac{\partial \tau_{xy}}{\partial x} + \frac{\partial \tau_{yy}}{\partial y} + \frac{\partial \tau_{zy}}{\partial z} + \rho f_y \tag{3}$$

$$\frac{\partial(\rho w)}{\partial t} + \nabla.(\rho w V) = -\frac{\partial p}{\partial z} + \frac{\partial \tau_{xz}}{\partial x} + \frac{\partial \tau_{yz}}{\partial y} + \frac{\partial \tau_{zz}}{\partial z} + \rho f_z \tag{4}$$

$$\begin{aligned}\frac{\partial}{\partial t}\left[\rho\left(e+\frac{v^2}{2}\right)\right] + \nabla\cdot\left[\rho\left(e+\frac{v^2}{2}\right)V\right] = \rho\dot{q} + \frac{\partial}{\partial x}\left(k\frac{\partial T}{\partial x}\right) + \frac{\partial}{\partial y}\left(k\frac{\partial T}{\partial y}\right) + \frac{\partial}{\partial z}\left(k\frac{\partial T}{\partial z}\right) - \\ \frac{\partial(up)}{\partial x} - \frac{\partial(vp)}{\partial y} - \frac{\partial(wp)}{\partial z} + \frac{\partial(u\tau_{xx})}{\partial x} + \frac{\partial(u\tau_{yx})}{\partial y} + \frac{\partial(u\tau_{zx})}{\partial z} + \frac{\partial(v\tau_{xy})}{\partial x} + \frac{\partial(v\tau_{yy})}{\partial y} + \frac{\partial(v\tau_{zy})}{\partial z} + \\ + \frac{\partial(w\tau_{xz})}{\partial x} + \frac{\partial(w\tau_{yz})}{\partial y} + \frac{\partial(w\tau_{zz})}{\partial z} + \rho f\cdot V\end{aligned} \tag{5}$$

Where,

ρ: density;
t: time;
V: velocity vector;
u: velocity's x-component;
v: velocity's y-component;
w: velocity's z-component;
τ: shear stress;
p: pressure.
f: body force vector;
e: internal energy;
q: heat flux vector;
k: thermal conductivity;
T: temperature.

Equation (1) is relative to the mass conservation, while Eq. (2) to Eq. (4) are the x, y and z components of the momentum conservation equation, respectively, and Eq. (5) represents the energy conservation written in terms of total energy.

Although these equations in conservation form, describe fluid flow in a generic domain, a turbulence model is also necessary to solve time-dependent fluctuations regarding non-laminar flows which are characterized by significant inertial terms relative to viscous terms. The Reynolds number, which is a dimensionless number, is often used to quantify these physical terms rates for flow problems.

$$\mathrm{Re}=\frac{\rho v L}{\mu} \tag{6}$$

Where,

L: characteristic length;
μ: dynamic viscosity;

The velocity and all other flow properties vary in a random and chaotic way with a wide range of length and time scales. For example, the range of eddy sizes that might be found in fluid flow is shown schematically on the left-hand of Fig. 2. The right hand side of this figure shows the time history of a typical velocity component at a point in the flow. Therefore, the turbulence level in the fluid domain should be analyzed in terms of Reynolds number in order to choose the adequate turbulence model and its length and time-scale treatment.

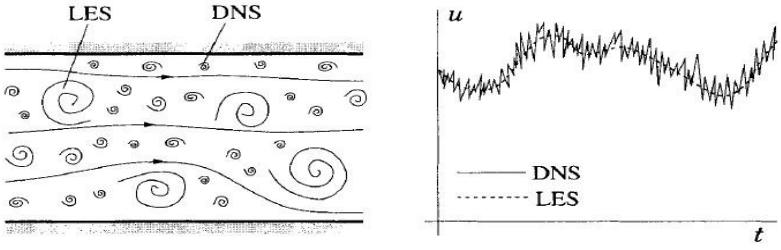

Figure 2. Schematic representation of turbulent motion (left) and the time dependence of a velocity component at a point (right) (Ferziger and Peric, 2002)

Using the fluid flow governing equations shown previously, a discretization method is applied to the domain. For CFD problems, the Finite Volume Method (FVM) is commonly used, where the domain is subdivided into small control volumes (mesh) and the governing equations in conservation laws are applied to obtain the numerical solution. Some of the possible volume controls are presented in Fig. 3.

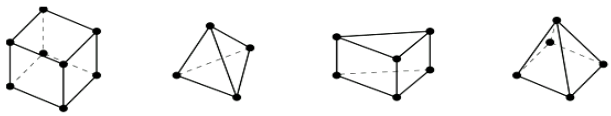

Figure 3. Types of control volumes (from left to right: hexahedral, tetrahedral, prism and pyramid)

All of these CFD techniques are included in a commercial code such as the ANSYS package. This code, like some others commercial codes, has a pre-processor, on which the mesh generation and boundary conditions are generated and applied. It also includes a solver module which solves the equations for the domain. Furthermore a post-processor is included and is used to analyze the results including pressure and velocity field.

2. MATERIALS AND METHODS

2.1. Experimental data

The experimental data obtained using the laboratory quench system shown in Fig. 4. The blue portion of fig. 4 represents the pump which provides quenchant agitation during cooling process when the steel test bars are immersed

into the quench tanks. The quench tanks are illustrated as two silver-colored cylinders in Fig. 4. The remaining parts are valves, tubes, and the wireframe structure.

AISI 304 stainless steel was the material used as the cylindrical test bar to aquire cooling curves for both water and oil baths with different agitation and temperature flows. The thermocouple was placed in a radial position. The sample dimensions as well the thermocouple locations are also shown in Fig. 4.

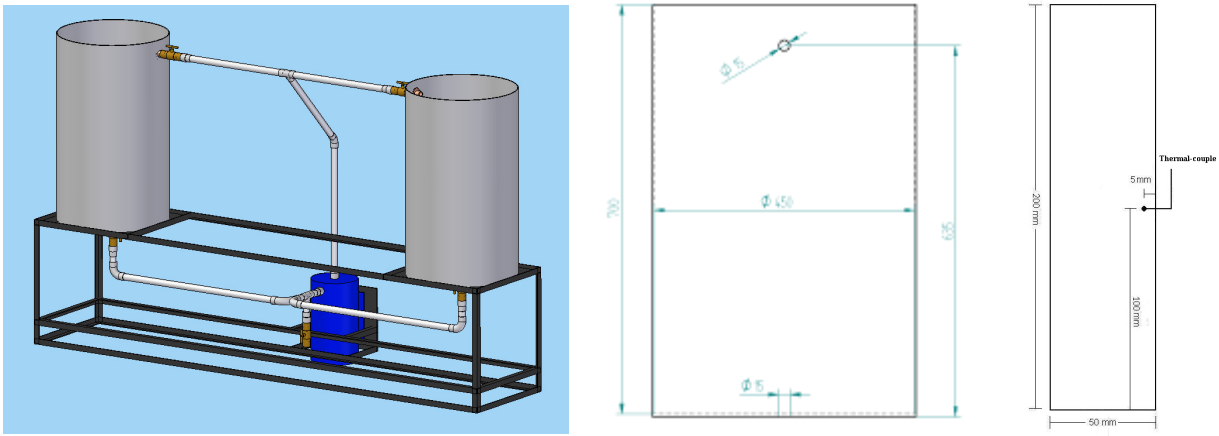

Figure 4. Quench system assembly (left) quench tank dimensions (center) and thermocouple position into sample (right, dimensions in mm).

For the experiment quenching data was acquired using a single bath temperature of 40°C, and two of mass flow rate were used which are shown in Table 1.

Table 1. Operating conditions for the quenching experiment.

Fluid	Simulation	Mass flow rate [kg/s](1)
Water	WM1	0.624
	WM2	1.247
Oil	OM1	0.624
	OM2	1.247

(1): measured at the tank inlet

2.1.1. Quenching

For water and oil quenching, the steel test probes were heated to an initial value of 800°C. Cooling curves obtained at 40˚C to the agitation rates shown in Table 1 are illustrated in Fig. 5.

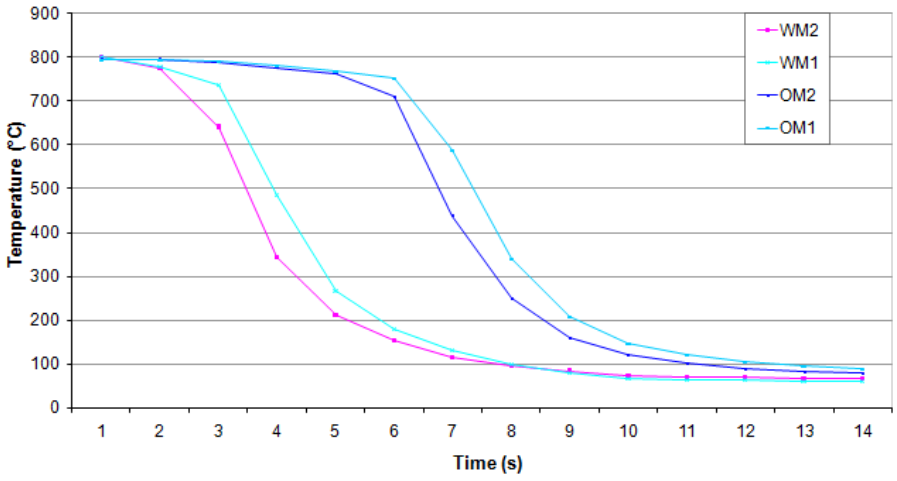

Figure 5. Cooling curves obtained for oil and water quenching at different operating conditions.

As shown in Fig. 5, temperature has no significant changes after 12s. Therefore, a value of approximately 15s was used as the total time for the CFD simulations.

2.2. CFD Pre-processing

Virtual geometry was generated using ANSYS ICEM CFD software which was also used for mesh generation. After domain discretization, the simulation and analysis of the results was performed using ANSYS CFX-Solver (solver for initial and boundary conditions at the domain) and ANSYS CFX-Post (post-processing results).

Quench system geometry was recreated using a 3-dimensional model for CFD simulations as shown in Fig. 6.

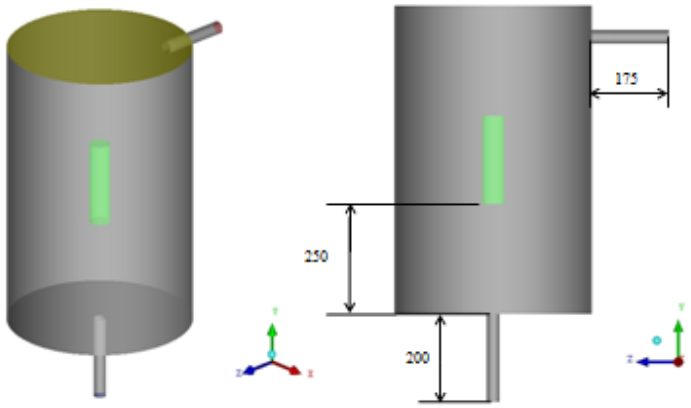

Figure 6. Virtual quench tank with metal sample inside (dimensions in mm).

The geometry includes quench tank, metal sample (test probe) and small portions of inlet and outlet pipes to guarantee the velocity direction in these regions, especially at tank inlet.

A hexahedral mesh, which is highly recommended for convective driven flows, was generated for the fluid and solid domains.

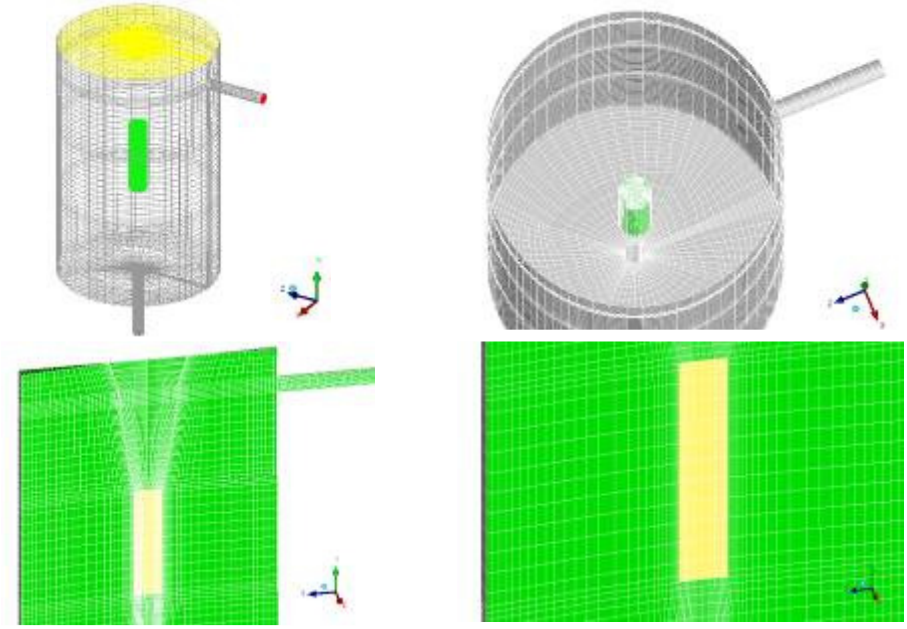

Figure 7. Hexahedral mesh generated in the fluid and solid domains with 200.000 elements.

For problem simplifications, some considerations were assumed regarding boundary conditions. At the domain top surface, which correspond to the free-surface fluid flow during experimental simulation, was imposed on the wall with free-slip velocity to assure no shear stress at this surface.

Although boiling influences the cooling, it generally occurs into first five seconds (for the test probe and quenching conditions used here) and is not a significant factor in fluid flow for the total time to be modeled by the simulation.

Therefore, some computed temperature results around the probe may not coincide with experimental data during the initial simulation period. All other information regarding the simulation setup is shown in Tab. 2.

Table 2. Setup for CFD simulations.

Simulation Type	Total Time [s]	Timesteps [s]	Reference Pressure [atm]	Turbulence model	Residual target	Outlet boundary condition	Tank walls boundary conditions
Transient	15	0.05	1	Shear Stress Transport (SST)	1e-05	Average Relative Static Pressure of 0 atm	Adiabatic walls

3. RESULTS

Results for velocity and temperature fields for both quenchants are presented in Figs 8 and 9, at YZ cut plane and for simulation time of 1, 5, 10 and 15 seconds.

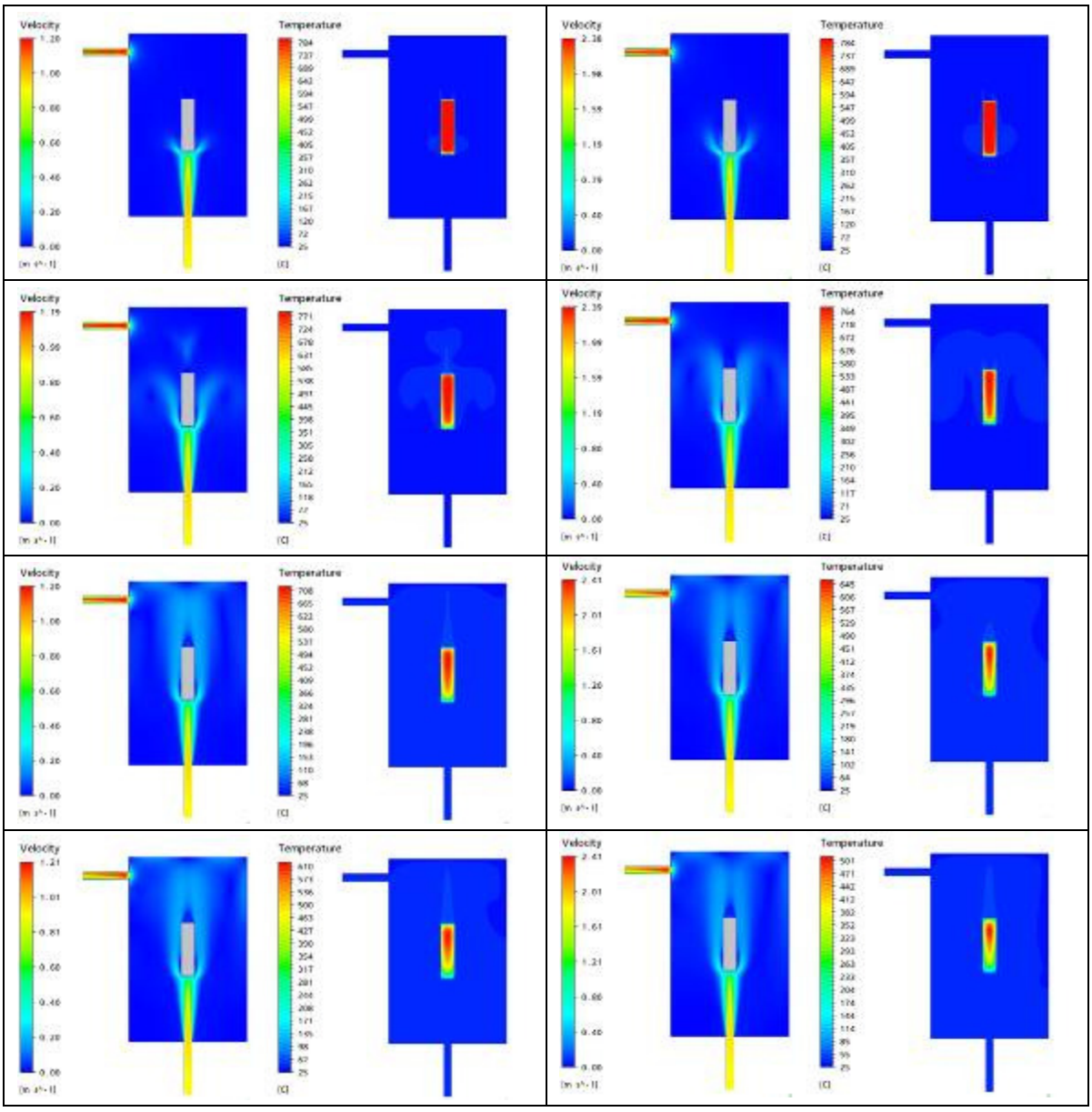

Figure 8. Contours of velocity and temperature at 1, 5, 10 and 15s (top-down) for simulation WM1, on left, and for simulation WM2, on right side

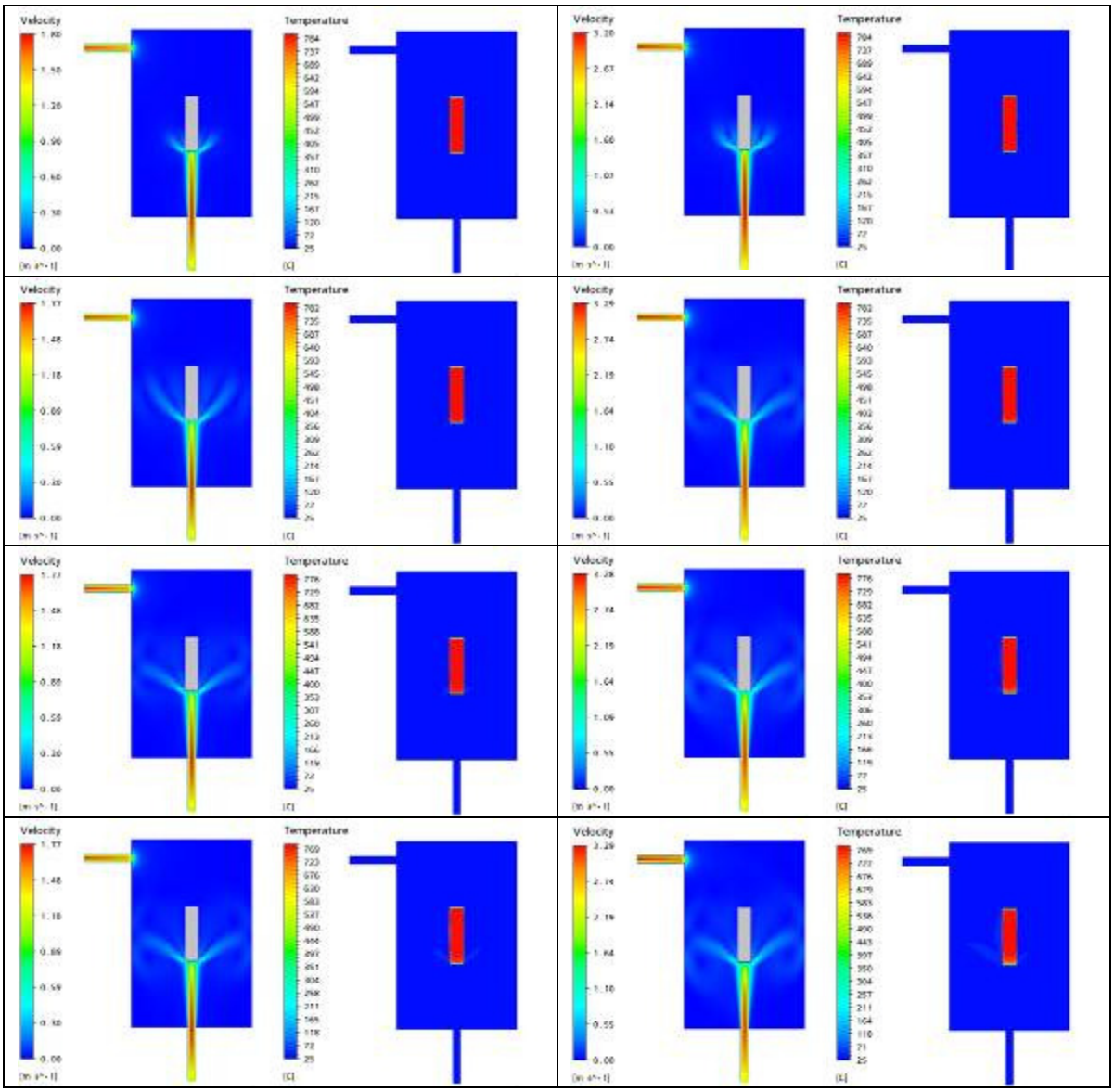

Figure 9. Contours of velocity and temperature at 1, 5, 10 and 15s (top-down) for simulation OM1, on left, and for simulation OM2, on right side

4. CONCLUSIONS

Experimental data shows higher cooling rates for water quenching relative to the oil quenching process. These results are due to the specific heat of water which is more than two times the value used for the oil quenchant (2000 J/kg.K). This difference between water and oil quenchant was expected.

In addition, as shown in Fig. 8, the velocity flow field for water quenching seems more uniform around the steel probe than that observed for the oil quenching process shown in Fig. 9. The non-uniformity flow field for oil, under these simulation conditions, is due to the viscosity (0.0725 kg/m.s) of the quench oil which is much higher than water.

As a result of these different material properties and even with the same simulation conditions and experimental tests, the oil quenching process should be improved to assure higher cooling rates comparable to those obtained for the water quenchant, if this quenchant is preferred.

An estimate for the necessary oil agitation may be provided by the Reynolds number shown in Eq. (6). For these simulations, the Reynolds number for water quenching is about 135000 and for oil, a value around 1820 is calculated. To obtain comparable quenching results, comparable Reynolds numbers should be used. However, for these conditions, it's experimentally impossible to match, because the oil inlet velocity would necessary be required to be 244 m/s which is not possible as the equipment is currently constructed.

The water quenching process obtained for this experimental system configuration shows the best way to obtain fluid flow uniformity around the sample is to provide better heat exchange between metal surface and fluid.

5. REFERENCES

ANDERSON JUNIOR, 1995, J.D. Computational Fluid Dynamics: The basics with applications. McGraw-Hill, Inc. New York, NY, USA, 547 p.

ANSYS, Inc., 2006, ANSYS CFX-Solver – Theory Guide, Release 11.0. Canonsburg, PA, December, 312 p.

ASM, 1977. Atlas of Isothermal Transformation and Cooling Transformation Diagrams.

BANKA, A. L., 2005, Practical Applications of CFD in Heat Processing. HEAT TREATING PROGRESS, August, pp. 44-49.

BARTH, T., 2003, Numerical Methods for Conservations Laws on Structured and Unstructured Meshes. VKI March 2003 Lecture Series. NASA Ames Research Center, Moffet Field, California 94035, USA, 65 p.

BERGMAN, H. R., 1970, Importance of Agitation for Optimum Quenching. Report presented in the ASM Materials Engineering Congress, 19-22 Oct, 15 p.

FERZIGER, J. H., PERIC, 2002, M. Computational Methods for Fluid Dynamics. Springer, New York, USA, 423 p.

HECK, U., FRITSCHING, U., BAUCKHAGE, K., 2001, Fluid flow and heat transfer in gas jet quenching of a cylinder. International Journal of Numerical Methods for Heat and Fluid Flow, 11, 1,. pp. 36-49

KOCK, D. J., CRAIG, K. J., SNYMAN, J. A., 2000, Using mathematical optimization in the CFD analysis of a continuous quenching process. International Journal for Numerical Methods in Engineering, 47, pp. 985-999.

MANIRUZZAMAN, M., SISSON JUNIOR, R.D., 2004, Heat transfer coefficients for quenching process simulation. Journal de physique, IV, France, 120, pp. 521-528.

RONDEAU, D., 2006, The effects of part orientation and fluid flow on heat transfer around a cylinder. A Thesis Submitted to the Faculty of Worcester Polytechnic Institute. New England, USA. May 6, 75 p.

TOTTEN, G. E., LALLY, K. S. Proper agitation dictates quench success. Part 1. HEAT TREATING, Sep 1992, 12 p.

VERSTEEG, H. K., MALALASEKERA, W., 1995, An Introduction to Computational Fluid Dynamics – The Finite Volume Method. Longman Scientific & Technical, England, 257 p.

6. RESPONSIBILITY NOTICE

The authors are the only responsible for the printed material included in this paper.